

# DESY SUMMER STUDENT PROJECT



**Bc. Martin Ďurišin**

*(DESY summer student 2009)*

*Date of birth:*

March 30, 1987

*Nationality:*

Slovak

## **Deformation of metallic glasses studied by high-energy X-ray diffraction**

*Area of research:*

Photon Physics, Material Science

*Time frame:*

July 21 – September 10, 2009



*Supervisor:*

Dr. Jozef Bednarcik

Deutsches Elektronen Synchrotron DESY

Notkestr. 85

22607 Hamburg, Germany

email: [jozef.bednarcik@desy.de](mailto:jozef.bednarcik@desy.de)

phone: +49-40-89981861

## Short description of the research project

The main objective of this project was to follow the strain distribution within  $\text{Cu}_{45}\text{Zr}_{46.5}\text{Al}_{17}\text{Ti}_{1.5}$  bulk metallic glass undergoing bend deformation using in-situ hard X-ray diffraction. The special emphasis was placed at the observation of differences between the strain distributions within  $\text{Cu}_{45}\text{Zr}_{46.5}\text{Al}_{17}\text{Ti}_{1.5}$  bulk metallic glass when exposed to different levels of bending deformation. X-ray diffraction experiments using high-energy photons (100 keV) were performed at the BW5 wiggler beamline of DORIS III positron storage ring at DESY.



## Contents

<b>1</b>	<b>Introduction</b>	<b>1</b>
<b>2</b>	<b>Goals of the research project</b>	<b>1</b>
<b>3</b>	<b>Experimental part</b>	<b>2</b>
3.1	Preparation of samples . . . . .	2
3.2	High-energy X-ray diffraction at BW5 . . . . .	2
3.3	Data treatment . . . . .	4
<b>4</b>	<b>Results and Discussion</b>	<b>6</b>
<b>5</b>	<b>Conclusions</b>	<b>8</b>
	<b>Acknowledgement</b>	<b>8</b>
	<b>References</b>	<b>8</b>

## 1 Introduction

Bulk metallic glasses (BMGs) represent relatively new class of materials which exhibit many interesting properties[1]. These multi-component metallic alloys can be obtained at low cooling rates, which allow the production of large-scale materials, by conventional casting processes [2]. Compared with crystalline counterparts, bulk metallic glasses (BMGs) have some superior properties, such as high yield strength, hardness, large elastic limit, high fracture toughness and corrosion resistance, and hence are considered as promising engineering materials [1, 3]. BMGs have strengths approaching the theoretical limit [4] but their plasticity at room temperature is typically very low. For the majority of the known BMGs, the plastic strain at room temperature is very limited ( $< 2\%$ ) even under compression, resulting from pronounced shear localization and work softening. The lack of plasticity makes BMGs prone to catastrophic failure in load-bearing conditions and restricts their application.

High-energy X-ray diffraction (XRD) has proven to be a suitable tool to describe the local atomic structure of the metallic glasses [5]. It was recently demonstrated that high-energy X-ray scattering can be used to measure the elastic strain under compression [6, 7] and tension [8, 9].

## 2 Goals of the research project

The main objective of this project is to follow the strain distribution within Cu-based bulk metallic glass when exposed to different levels of bend deformation using in-situ hard X-ray diffraction. Particular goals can be formulated as follows:

- perform high-energy X-ray diffraction experiments on  $\text{Cu}_{45}\text{Zr}_{46.5}\text{Al}_{17}\text{Ti}_{1.5}$  bulk metallic glass during bending,
- determine the strain distribution along the sample width,
- compare the strain distributions for the two different bending radii (10 and 20 mm).

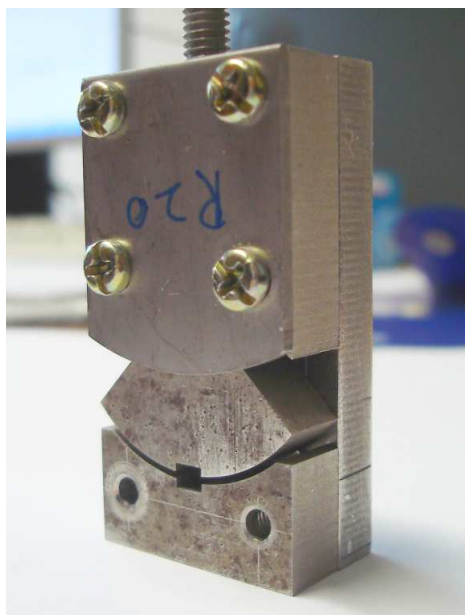


**Figure 1:** Bending device used in this study for bending of  $\text{Cu}_{45}\text{Zr}_{46.5}\text{Al}_{17}\text{Ti}_{1.5}$  bulk metallic glass.

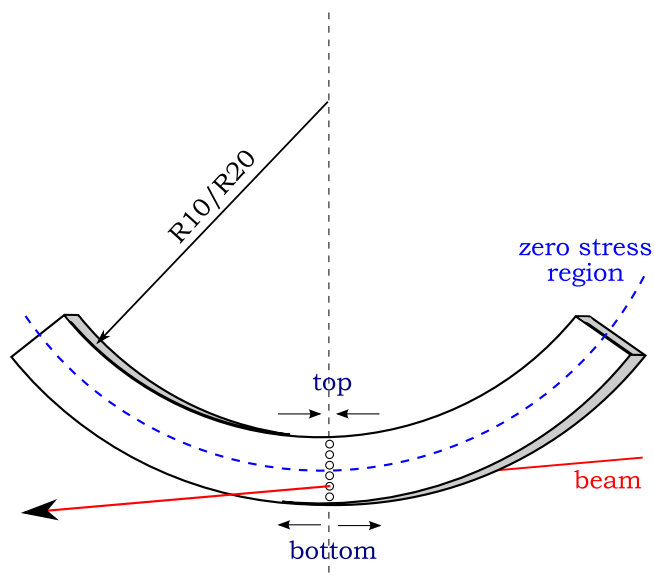


**Figure 2:** Schematic drawing showing bending geometry and area (depicted by circles) which was investigated using high-energy X-ray diffraction.

### 3 Experimental part

#### 3.1 Preparation of samples

Bulk metallic glasses with nominal composition of  $\text{Cu}_{45}\text{Zr}_{46.5}\text{Al}_{17}\text{Ti}_{1.5}$  (at. %) were prepared by copper mould casting. Samples were further polished in order to prepare bar-shaped pieces having the length, width and thickness of 30, 1 and 0.5 mm, respectively. In total two identical samples were prepared. Samples were further bent to different levels using two benders having bending radii of 10 (R10) and 20 mm (R20), respectively. Figure 1 shows bender having bending radius of 20 mm (R20). Figure 2 shows schematic drawing showing specimen undergoing bending deformation. I would like to add that samples and benders were prepared in group of Prof. J.Z. Jiang<sup>1</sup>.

#### 3.2 High-energy X-ray diffraction at BW5

Wiggler beamline BW5 can produce photon beams with energies ranging between 60 and 150 keV. This facility is dedicated to X-ray scattering experiments. Due to high penetration depth of high energy photons, bulk samples having thickness several mm (depending on material composition) can be investigated in transmission mode. Synchrotron radiation at the BW5 station is produced by wiggler, which emits high-energy

<sup>1</sup>International Center for New-Structured Materials ICNSM, Zhejiang University and Laboratory of New-Structured Materials, Department of Materials Science and Engineering, Zhejiang University, Hangzhou 310027, P.R. China

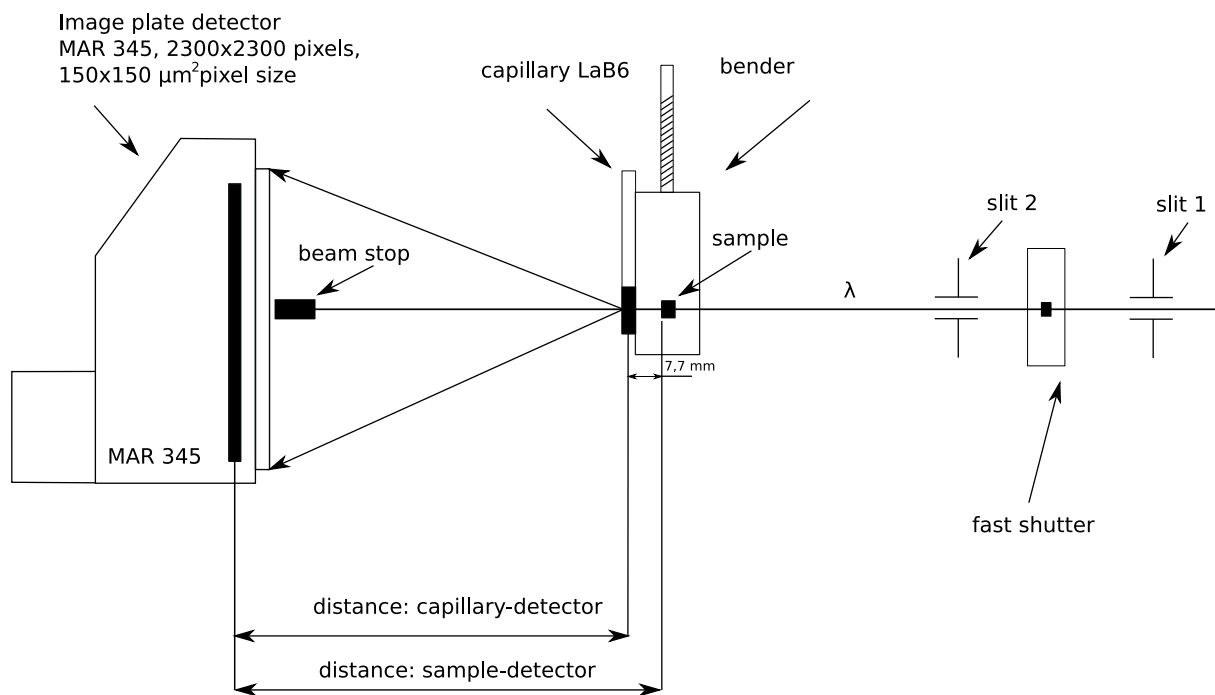


**Figure 3:** Schematic drawing of the experimental setup at wiggler BW5 beamline used for room temperature high-energy X-ray diffraction on bulk metallic glasses.

photons in a relatively wide horizontal fan. To minimize beam losses due to air scattering all beam guide pipes are evacuated. Polychromatic photon beam is further guided down stream to collimator. The role of the collimator is to define the shape and size of incoming polychromatic photon beam. Since collimator is exposed to instantaneous radiation it has to be cooled down in order to prevent its melting due to high thermal load. The central part of the collimator consist of W (tungsten) plate having whole which defines the profile of the incoming beam. During our experiments we used square-shaped opening with  $1 \times 1 \text{ mm}^2$  size. Figure 3 shows arrangement of all components during X-ray diffraction experiments at BW5. After collimation the polychromatic beam is further guided to monochromator. In our experiments we used gradient Ge-Si(111) single crystal to monochromatize polychromatic beam. Two pairs of slits represent an important component which helps to control beam profile and also suppress parasitic air scattering. A fast shutter allows time-controlled exposures. The sample loaded into bender is placed on the sample tower and can be positioned with respect to the beam. Incoming beam is partly diffracted on sample. Diffracted photons are collected using two-dimensional image plate detector MAR345. The image plate has a  $0.4 \text{ mm}$  coating of  $\text{BaFBr:Eu}^2$  which converts invisible X-rays into visible light. This detector has resolution  $2300 \times 2300$  pixels and each pixel has a size of  $150 \times 150 \text{ } \mu\text{m}^2$ . The data are digitized and converted into a square pixel array. Typical readout when using such resolution is about  $100 \text{ s}$ . The sample-detector distance was calibrated using X-ray diffraction measurement on  $\text{LaB}_6$  powder, which was inserted into quartz capillary. During experiments

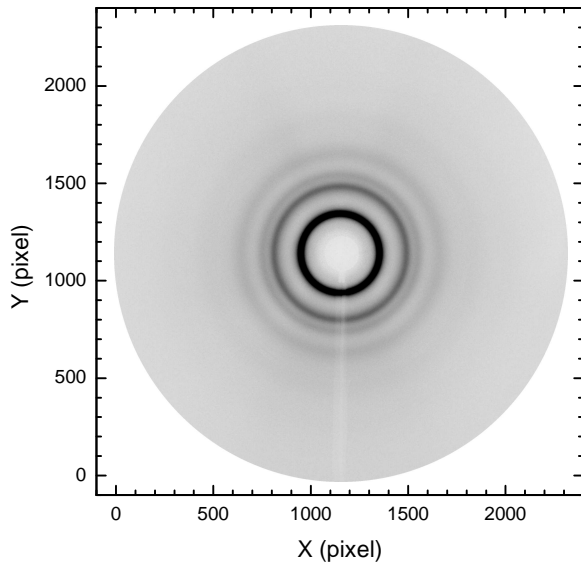


**Figure 4:** Diffuse diffraction pattern of fully amorphous  $\text{Cu}_{45}\text{Zr}_{46.5}\text{Al}_{17}\text{Ti}_{1.5}$  bulk metallic glass.

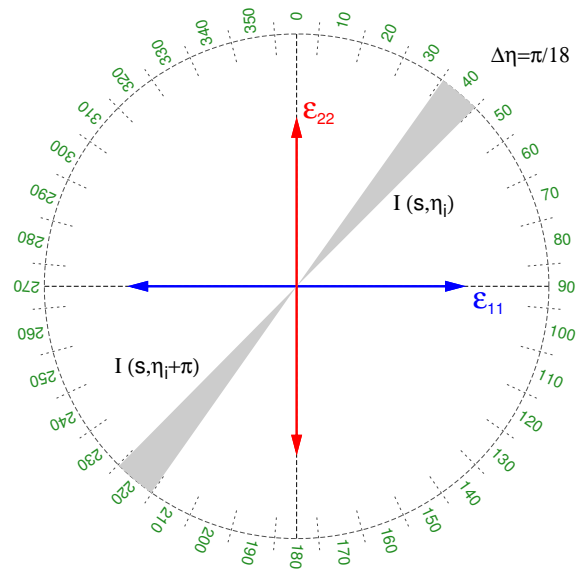


**Figure 5:** Schematic sketch depicting polar coordinate system and so called "caking" of two-dimensional diffraction patterns.

the beam energy was set to 100 keV which equals to wavelength  $\lambda = 0.12384 \text{ \AA}$ . The beam cross section was set to  $1 \times 0.1 \text{ mm}^2$ . As can be seen from Fig.2, central part of specimen undergoing bending deformation was scanned as indicated by open circles. The step size was 0.1 mm. In total about 10 different position were scanned. To improve overall statistics, about seven independent scans were taken from each position along the sample width.

### 3.3 Data treatment

The strain determination of bulk metallic glasses from x-ray diffraction data is based on concepts previously reported by Poulsen *et al.* [6]. Figure 4 shows an example for the raw data obtained for the  $\text{Cu}_{45}\text{Zr}_{46.5}\text{Al}_{17}\text{Ti}_{1.5}$  bulk metallic glass. The symmetric circular diffraction pattern is characterized with respect to the polar coordinates  $(s, \eta)$ . By dividing the  $\eta$ -range of 0 to  $2\pi$  into 36 segments, one obtains symmetrized intensity distributions

$$I'_i(q, \eta_i) = \int_{\eta_i - \pi/36}^{\eta_i + \pi/36} [I(q, \eta) + I(q, \eta + \pi)] d\eta \quad (1)$$

with  $\eta_i = i\pi/18$ ,  $i = 0 \dots 17$ , where the amplitude of the wave-vector transfer  $q = q(s)$  is defined by

$$q(s) = \frac{4\pi}{\lambda} \sin \left[ \frac{1}{2} \arctg \left( \frac{s}{D} \right) \right] \quad (2)$$

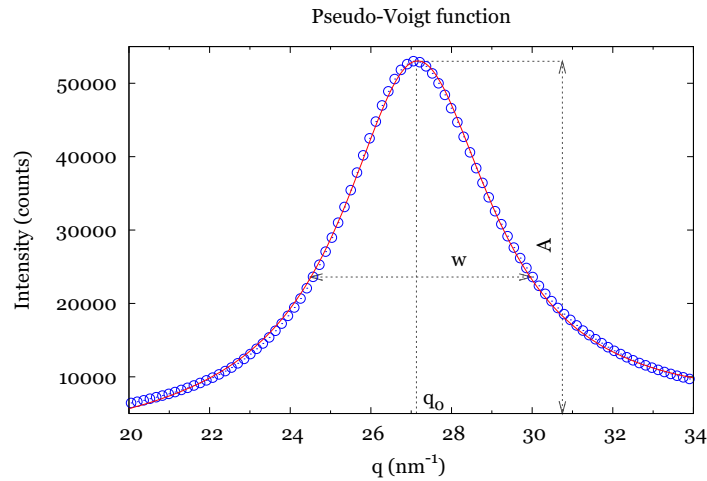


**Figure 6:** Profile modelling of the principal diffuse peak using Pseudo-Voigt function, described by equation (3).

in which  $\lambda$  denotes the wavelength,  $D$  refers to the sample-to-detector distance and  $s$  represents the distance from the origin of the polar coordinate system. Symmetrized intensity distributions as described by eq. (1) were calculated using the software package FIT2D [10]. The procedure was repeated for all diffraction patterns acquired at different positions thus yielding the set of symmetrized distributions  $I'_i(q, \eta_i, z)$  where  $z$  refers to the corresponding position within bending region (indicated by open circles in Fig.2). The profile of the first (principal) diffraction peak appearing in each  $I'_i(q, \eta_i, z)$  was modelled assuming linear background and pseudo-Voigt function  $I_P(x)$  having the analytical form

$$I_P(x) = A [\alpha C(x) + (1 - \alpha)G(x)], \quad (3)$$

where  $A$  is amplitude,  $C(x) = (1 + x^2)^{-1}$  represents Cauchy and  $G(x) = \exp[-(\ln 2)x^2]$  Gaussian part, with  $x = (q - q_0/w)$ , in which  $w$  is the full-width at half-maximum (FWHM),  $\alpha$  the Cauchy content and  $q_0$  the position of a peak maximum. The peak position  $q_0$  and other profile parameters were determined by nonlinear least-squares fit of pseudo-Voigt function to a set of data points corresponding to the principal diffraction peak. Since more data points are considered for determining peak position, the influence of the error of an individual data point on the peak position is minimized.

For each  $I'_i(q, \eta_i, z)$  the shift in position of the first (principal) peak,  $q_0(\eta_i, z)$ , was determined with respect to the peak position determined from the zero stress region,  $q_0(\eta_i, z_0)$ . The relative change of the position of the principal peak upon applying an external stress defines the strain [6, 7]

$$\epsilon_i(\eta_i, z) = \frac{q_0(\eta_i, z_0) - q_0(\eta_i, z)}{q_0(\eta_i, z)}. \quad (4)$$

(with  $\eta_i = i\pi/18$ ,  $i = 0 \dots 17$ ), which is angular dependent. The angular variation of

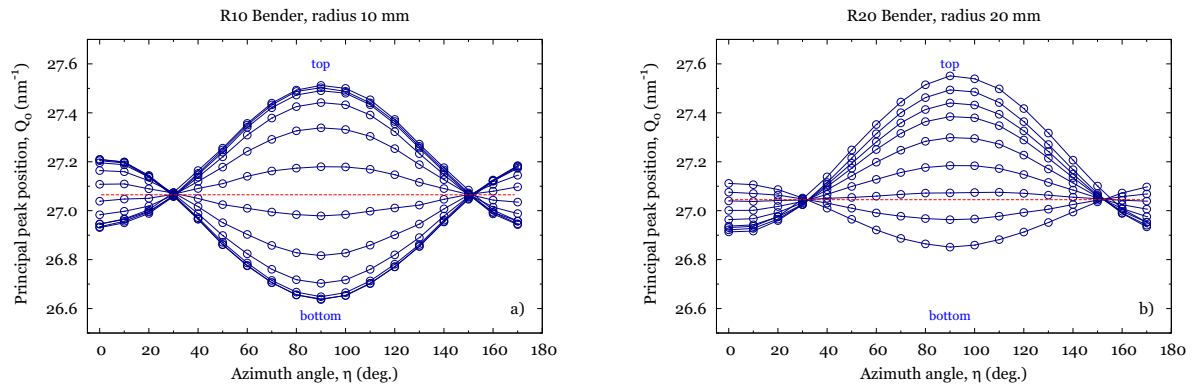


**Figure 7:** Angular dependence of the principal diffuse peak  $q_0$  along the sample width for the two different bending radii. The lines are just guides for eyes. The red lines connecting intersection points depict the zero stress region.

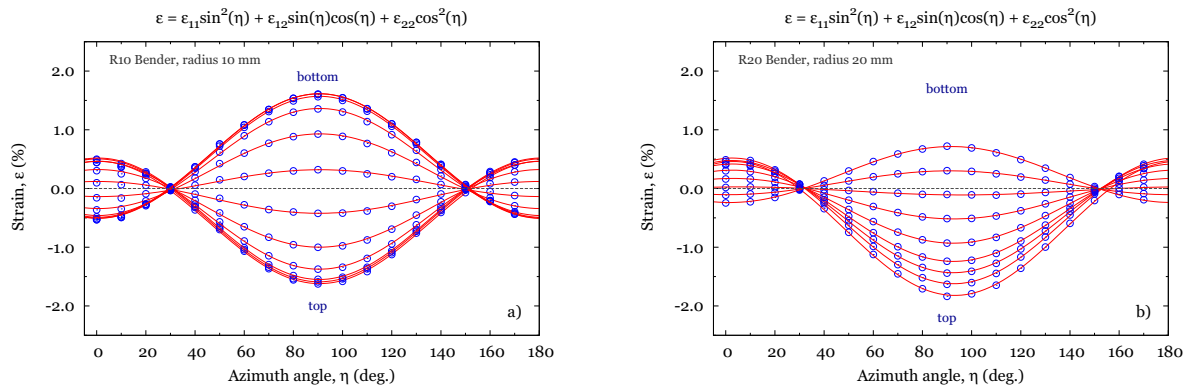


**Figure 8:** Angular dependence of the strain  $\epsilon$  along the sample width for the two different bending radii. The full lines represent fits of strain curves to the equation (5).

the strain can be fitted to the following expression [11]

$$\epsilon_i(\eta_i, z) = \epsilon_{11} \sin^2(\eta_i) + \epsilon_{12} \sin(\eta_i) \cos(\eta_i) + \epsilon_{22} \cos^2(\eta_i). \quad (5)$$

As a result, the strain tensor can be determined, and the axial ( $\epsilon_{11}$ ), tangential ( $\epsilon_{22}$ ) and in-plane shear component ( $\epsilon_{12}$ ) can be derived. Components not in the plane perpendicular to the incoming beam can be determined by rotating the specimen around an axis perpendicular to the incoming beam.

## 4 Results and Discussion

Figure 7 shows azimuth angle  $\eta$  dependence of the principal diffuse peak  $q_0$  along the sample width as obtained from the X-ray diffraction experiments on two bent samples using two different bending radii R10 and R20, respectively. It should be noted here that each line corresponds to a specific position along the sample width (see Fig.2). From



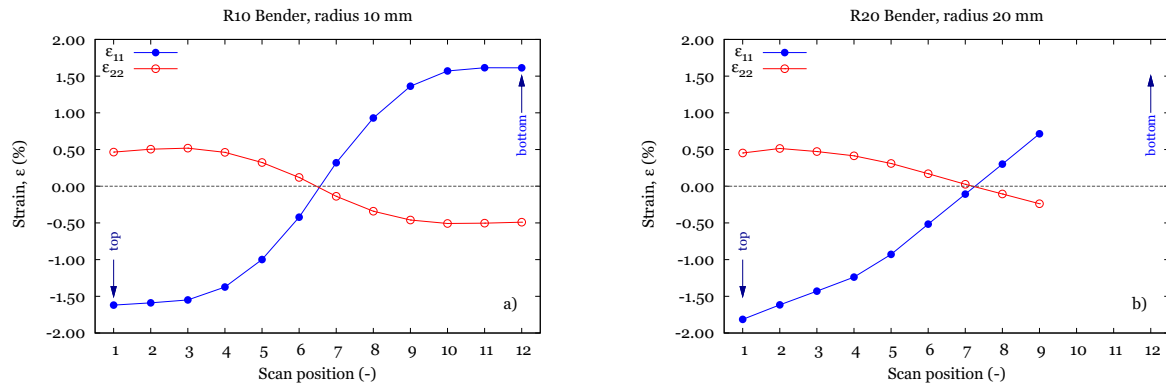


**Figure 9:** Position dependence of the strain tensor components  $\epsilon_{11}$  and  $\epsilon_{22}$  corresponding to the horizontal and vertical direction, respectively.

the first look both dependences show similar behavior. The maximum  $q_0$  appearing at the azimuth angle  $\eta = 90^\circ$  (horizontal direction, see Fig.5) from the top side gradually decreases and reaches minimum when approaching the bottom side of the sample. Since the position  $q_0$  of the principal diffuse peak is inversely proportional to the mean atomic spacing in amorphous material, one can conclude that the top part is in horizontal direction effectively compressed while the bottom side is effectively under tension. As can be further seen from Fig.7, all curves intersect in two distinct points, which define the zero stress region with the corresponding principal peak position  $q_0(\eta_i, z_0)$ . Furthermore one can see that the zero stress region is located in the middle of sample. I would like to add that missing curves for R20 bender are due to error in scanning macro which did not reached the bottom part of the sample and finished few steps earlier.

Knowing the principal diffuse peak positions  $q_0(\eta_i, z_0)$  corresponding to the zero stress region, dependences shown in Fig.7 can be converted to strain curves using equation (4). Fitting strain curves to the equation (5) strain tensor components  $\epsilon_{11}$  and  $\epsilon_{22}$  corresponding to the horizontal and vertical direction, respectively, were determined.

Figure 9 shows Position dependence of the strain tensor components  $\epsilon_{11}$  and  $\epsilon_{22}$  along the sample width. This data confirm that the top part of the investigated region is in horizontal direction effectively compressed and reveals maximum compressive strain  $\epsilon_{11}$  of 1.62 and 1.81 % for R10 and R20 bender, respectively. On the other side the very bottom part is under tension. Transversal strains  $\epsilon_{22}$  have opposite signs and exhibit much lower amplitudes. All dependences show symmetric behavior and confirm that the zero stress region lays within the central part of the specimen.

## 5 Conclusions

In this study we showed that X-ray diffraction using high-energy photons is powerful technique to describe the deformation state of  $\text{Cu}_{45}\text{Zr}_{46.5}\text{Al}_{17}\text{Ti}_{1.5}$  bulk metallic glass. Doing fine scans on BMG sample exposed to bending deformation revealed that the upper part is in horizontal direction effectively compressed whereas the bottom part is effectively stretched. Comparing results for two different bending radii we found that the zero stress region lays within the central part of the specimen. Furthermore, larger bending radius implies bit larger amplitudes for  $\epsilon_{11}$  strains and smoother strain gradient along the specimen width.

## Acknowledgement

I would like to render thanks all people and colleagues from High-energy X-ray scattering group who help me with my work at DESY. Especially my supervisor Dr. Jozef Bednarcik and his DAAD fellow Štefan Michalik who had patience to help me with any problems. I would like to thanks Prof. J.Z. Jiang who provided us with samples and benders for our experiments. Big thanks belong to DESY allowing me to participate at the DESY Summer Student Program 2009.

## References

- [1] A. Inoue, *Acta Materialia* **48** (2000) 279.
- [2] A. Inoue, A. Takeuchi, *Mater. Trans. JIM* **43** (2002) 1892.
- [3] W.L. Johnson, *MRS Bull.* **24** (1999) 42.
- [4] A.L. Greer, *Science* **267** (1995) 1947.
- [5] T. Egami T., S.J.L. Billinge, *Underneath the Bragg Peaks: Structural analysis of complex materials*, Pergamon Press, Elsevier, Oxford, England, 2003.
- [6] H.F. Poulsen, J.A. Wert, J. Neuefeind, V. Honkimäki, M. Daymond, *Nat. Mater.*, **4** (2005) 33.
- [7] T.C. Hufnagel, R.T. Ott, J. Almer, *Phys. Rev. B*, **73** (2006) 064204.
- [8] X.D. Wang, J. Bednarcik, K. Saksl, H. Franz, Q.P. Cao and J.Z. Jiang, *Appl. Phys. Lett.* **91** (2007) 081913.
- [9] X.D. Wang, J. Bednarcik, H. Franz, H.B. Lou, Z.H. He, Q.P. Cao, J.Z. Jiang, *Appl. Phys. Lett.* **94** (2009) 011911.
- [10] A.P. Hammersley, S.O. Svensson, M. Hanfland, A.N. Fitch, D. Häusermann D., *High Press. Res.*, **14**(1996) 235.
- [11] G.E. Dieter, *Mechanical Metallurgy*, 3rd ed. McGraw-Hill, London, (1988) p.44.